0090-9556/08/3603-508–516$20.00
DRUG METABOLISM AND DISPOSITION
Vol. 36, No. 3
19299/3305266
DMD 36:508–516, 2008
Printed in U.S.A.
Copyright © 2008 by The American Society for Pharmacology and Experimental Therapeutics

DMD
DRUG METABOLISM AND DISPOSITION
aspet

Characterization and Comparative Studies of Zebrafish and Human Recombinant Dihydrofolate Reductases—Inhibition by Folic Acid and Polyphenols

Tseng-Ting Kao, Kuan-Chieh Wang, Wen-Ni Chang, Chia-Ying Lin, Bing-Hung Chen, Hua-Lin Wu, Guey-Yueh Shi, Jen-Ning Tsai, and Tzu-Fun Fu

Department of Medical Laboratory Science and Biotechnology, College of Medicine, National Cheng Kung University, Tainan, Taiwan (T.-T.K., K.-C.W., W.-N.C., C.-Y.L., T.-F.F.); Faculty of Biotechnology, Kaohsiung Medical University, Kaohsiung, Taiwan (B.-H.C.); Department of Biochemistry and Molecular Biology, College of Medicine and Cardiovascular Research Center, National Cheng Kung University, Tainan, Taiwan (H.-L.W., G.-Y.S.); School of Medical Laboratory and Biotechnology, Chung Shan Medical University, Taichung, Taiwan (J.N.T.)

Received October 17, 2007; accepted November 30, 2007

ABSTRACT:

Dihydrofolate reductase (DHFR) catalyzes folic acid reduction and recycles dihydrofolate generated during dTMP biosynthesis to tetrahydrofolate. DHFR is the main target of methotrexate, the most widely used agent for antifolate therapy. Nevertheless, the emergence of methotrexate-resistance has greatly impeded the curative potential of this drug. Therefore, drugs with improved efficacy are still in demand, as well as an efficient in vitro assay system and animal model for antifolate drug discovery. The aim of this study is to evaluate the suitability of using zebrafish DHFR as an alternative assay system for antifolate drug discovery. The cDNAs encoding zebrafish and human DHFR were cloned, overexpressed, and purified. Similar structural and kinetic properties were revealed between zebrafish and human recombinant DHFRs. The susceptibilities of both enzymes to known DHFR inhibitors, including methotrexate and trimethoprim, and compounds with antifolate potential, such as polyphenols, are also comparable. In addition, the DHFR-mediated dihydrofolate reduction was significantly inhibited by its own substrate folic acid. An unexpected tissue-specific distribution of DHFR was observed with the highest level present in ova and brains of zebrafish. DHFR is also abundant in zebrafish embryos of early stages and decreased abruptly after 3 days postfertilization. The substantial resemblance between zebrafish and human DHFRs, as demonstrated in this study, provides compelling evidence supporting the use of zebrafish DHFR as an in vitro assay system for folate-related studies and drug discovery.

Dihydrofolate reductase (DHFR; 5,6,7,8-tetrahydrofolate:$NADP^+$ oxidoreductase; EC 1.5.1.3.) is a key enzyme in folate-mediated one-carbon metabolism. It catalyzes folic acid and dihydrofolate reduction, the only pathway that activates the oxidized form of folate coenzymes. DHFR participates in the biosynthesis of nucleic acids, proteins, neurotransmitters, vitamins, and *S*-adenosylmethionine. It is also the methyl group donor for most intracellular methylation reactions, including DNA methylation (Fig. 1). Alteration or inhibition of DHFR activity often causes profound effects on DNA stability and gene expression, leading to abnormal cell proliferation and embryogenesis, as well as many pathogeneses, including neural tube defects and cancer (Parle-McDermott et al., 2007). Several properties of DHFR, besides its vital role in maintaining folate pool homeostasis, have made this enzyme a favorite target of chemotherapy. DHFR is essential in a wide spectrum of microbial pathogens. DHFR is small in size, which allows for molecular modeling for effective drug design. In addition, DHFR is highly expressed in proliferating cells but barely detectable in normal human adult tissues. The later characteristic enables a differential inhibition against DHFR between normal and rapidly proliferating target cells, including cancer cells and replicating microbes (Gangjee et al., 2007). DHFR is the main target of methotrexate, an important chemotherapeutic agent used currently to treat several malignancies. Nevertheless, the often emerging methotrexate-resistance has impeded the curative potential of methotrexate. Therefore, great efforts are expected to be continuously devoted to developing new agents against DHFR with improved efficacy. Better understanding about DHFR and assays for antifolate drug screening are hence in demand.

The growing awareness in the pathogenesis associated with folate deficiency and the increased demand for folic acid supplementation also contribute to the recently renewed interest in DHFR. High doses of folic acid are often prescribed for pregnant women to prevent

Our sincere appreciation goes to Dr. Verne Schirch, Virginia Commonwealth University, for valuable advice and assistance. We also acknowledge the support from the grants funded by the Program for Promoting Academic Excellence of Universities, National Cheng Kung University (NCKU): Grant D96-3500 to T.-F.F. and Grant D96-2200 to H.-L.W., Director of Cardiovascular Research Center, NCKU.

Article, publication date, and citation information can be found at http://dmd.aspetjournals.org.

doi:10.1124/dmd.107.019299.

ABBREVIATIONS: DHFR, dihydrofolate reductase; PVDF, polyvinylidene difluoride; bp, base pair; GSE, grape seed extract; EGCG, epigallocatechin-3-gallate; RT-PCR, reverse transcription-polymerase chain reaction; IPTG, isopropyl β-D-thiogalactopyranoside; PAGE, polyacrylamide gel electrophoresis; hpf, hours postfertilization; dpf, days postfertilization.

Downloaded from dmd.aspetjournals.org at Kaohsiung Med Univ Lib on March 20, 2012

DMD
DRUG METABOLISM AND DISPOSITION
aspet

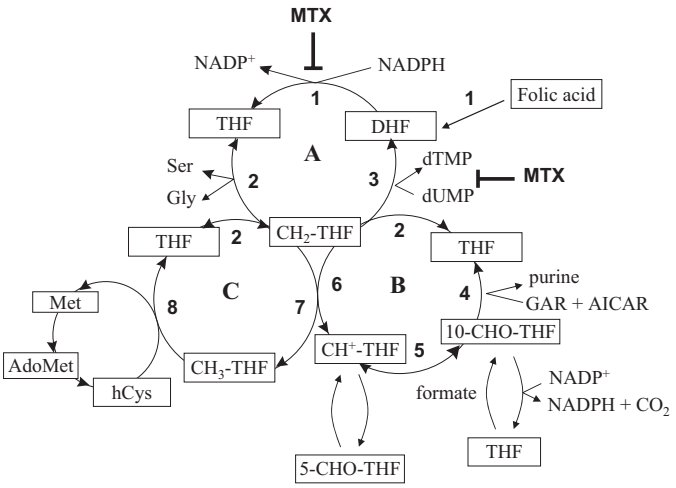

FIG. 1. Folate-mediated one-carbon metabolism involving dihydrofolate reductase. Three cycles are involved in this pathway and are responsible for thymidylate (A), purine (B), and methionine (C) biosynthesis. The enzymes participating in this pathway are dihydrofolate reductase (1), serine hydroxymethyltransferase (2), thymidylate synthase (3), glycinamide ribonucleotide transformylase (GAR) and 5-amino-4-imidazolecarboxamide ribotide transformylase (AICAR) (4), N^5,N^{10}-methenyltetrahydrofolate cyclohydrolase (5), N^5,N^{10}-methylenetetrahydrofolate dehydrogenase (6), N^5,N^{10}-methylenetetrahydrofolate reductase (7), and methionine synthase (8). AdoMet, *S*-adenosyl methionine; MTX, methotrexate; THF, tetrahydrofolate; DHF, dihydrofolate.

neural tube defects in the fetus. Ample amounts of folic acid are also ingested by the general population as a daily nutritional supplement. The beneficial effects of folate supplementation in preventing diseases have been well documented (Gisondi et al., 2007). However, detrimental effects of unmetabolized folic acid also appear, leading to a vigorous debate on mandatory folate fortification and supplement among researchers. Folic acid present in vitamin pills and fortified foods requires the action of DHFR to become fully reduced and metabolically active. Accumulated unmetabolized folic acid is transported into blood in a dose-dependent manner (Markle, 1997). Here it may bind to other folate enzymes and also act as an agonist of other intracellular biochemical reactions, causing pathogenesis and harmful effects to many biochemical systems (Troen et al., 2006). The properties and mechanism of DHFR catalysis hence warrants additional investigation, since DHFR is the enzyme responsible for metabolizing the oxidized form of folic acid in nutrient supplements.

The importance of an in vivo study can never be overemphasized, especially for drug discovery. Currently, the animal model employed for folate-related studies and antifolate drug development relies mostly on rodents for their resemblance with humans in folate-requiring enzymes. However, deciphering the role of folate enzymes in early mammalian development might be limited by the maternal contribution of folates during embryogenesis. Zebrafish is a recently emerging model prominent for human disease study and drug discovery. The feature of external development makes zebrafish a proper alternative for folate-related studies, since the maternal supply of folates and folate enzymes are likely to be depleted in the early stages of embryogenesis. Nevertheless, folate-mediated one-carbon metabolism and most folate enzymes, including DHFR, in zebrafish remain unexplored territory.

In this study, we clone and compare the recombinant zebrafish and human DHFRs to evaluate whether the zebrafish enzyme strongly resembles its human ortholog. The expression of DHFR in tissues and during embryogenesis is examined. The evidence to validate the use of zebrafish DHFR for antifolate drug development is also provided. In addition, we show that both zebrafish and human DHFR-mediated dihydrofolate reduction is inhibited by folic acid and polyphenol compounds to a similar extent, adding confidence to using zDHFR for potential antifolate drug screening. The physiological role of DHFR and clinical implication of DHFR inhibited by folic acid and polyphenols are also discussed.

Materials and Methods

Materials. PCR primers were ordered from MdBio, Inc. (Taipei, Taiwan). The SMART RACE amplification kit was purchased from Clontech (Mountain View, CA). PCR Master Mix was purchased from ABgene (Epsom, Surrey, UK). Enzymes used for cloning were purchased from Invitrogen (Carlsbad, CA) and New England Biolabs (Ipswich, MD). The high-performance liquid chromatography gel filtration column Alltech ProSphere SEC, 250 HR (4.6 mm × 30.0 cm), was purchased from Alltech (Lexington, KY). Polyvinylidene difluoride (PVDF) membranes were purchased from Millipore Corporation (Billerica, MA). Nickel-Sepharose resin slurry was purchased from Amersham Biosciences (Piscataway, NJ). Both the Bradford assay reagent and the BCA (bicinchoninic acid) Protein Assay kit were purchased from Pierce (Rockford, IL). Rabbit polyclonal anti-zDHFR antibody was produced by LTK Biolaboratories Inc. (Hsin-Chu, Taiwan) with the enzyme we provided. Horseradish peroxidase-conjugated goat anti-rabbit IgG was purchased from Santa Cruz Biotechnology (Santa Cruz, CA). The zebrafish liver epithelial cell line ZLE established by Miranda et al. (1993) was generously provided by Dr. Jiann-Ruey Hong, National Cheng Kung University, Taiwan. The IH636 grape seed extract, which was purchased from InterHealth Nutraceuticals (Benicia, CA), contains approximately 75 to 80% oligomeric proanthocyanidins and 3 to 5% monomeric proanthocyanidins (Shi et al., 2003). All other chemicals, including dihydrofolate, buffers, amino acids, and antibiotics, were purchased from Sigma-Aldrich (St. Louis, MO).

Fish Care and Preparation of cDNA Libraries. Zebrafish (*Danio rerio*, AB strain) were bred and maintained in a 10- to 14-h light-dark diurnal cycle following the standard procedure described by Westerfield (1995). Embryos were staged according to Kimmel et al. (1995). Total RNA isolation and cDNA library construction from zebrafish embryos and tissues and human Huh-7 cells were prepared with RNAzol B Reagent (Tel-Test Inc., Friendswood, TX) and the SMART RACE cDNA Amplification Kit as described previously (Chang et al., 2006).

Bacterial Strains, Plasmids, and General Cloning Procedures. The *Escherichia coli* strain XL1 Blue [*rec*A1, *end*A1, *gyr*A96, *thi-1*, *hsd*R17 (r_K^-, m_K^+), *sup*E44, *rel*A1, *lac*$^-$] was used for the construction of clones. The *E. coli* strain Rosetta (DE3) (F^- *ompT* $hsdS_B(r_B^-m_B^-)$ *gal dcm* (DE3)] containing the T7 RNA polymerase gene was used for protein expression. The pET43.1a plasmid and all the *E. coli* strains for cloning and expression were obtained from Novagen (Madison, WI). The materials and methods for the general cloning procedures were as previously described (Chang et al., 2006).

Cloning of DHFR Coding Sequences. Primers were designed based on the zebrafish DHFR cDNAs available in GenBank (accession number BC071330) to PCR amplify complete DHFR coding sequence from zebrafish 5′-RACE-Ready cDNA libraries. The primer sequences were 5′-GCGAAGTTCATCACATATGTCCCAGCGCAACGGTCATAC-3′ (forward) and 5′-GGACAGAGAATTCAAGCAGAAATGAGTTATAACTCTGGC-3′ (reverse) with introduced NdeI and EcoRI restriction enzyme sites to simplify the cloning procedures. The 500-bp PCR fragments were cloned into expression vector pET43.1a between NdeI and EcoRI sites, generating zDHFR/pET43.1a. For constructing His-tagged fusion zDHFR (zDHFR-His), we performed site-directed mutagenesis to remove the stop codon and introduce the XhoI site using zDHFR/pET43.1a as a template. This resulted in extension of six histidine residues at C terminus of DHFR proteins. The primers for site-directed mutagenesis were 5′-GC ATC AAA CAC TCA CTC GAG TTC CCG CGG-3′ (forward) and 5′-CC GCG GGA ACT CGA GTG AGT GTT TGA TGC-3′ (reverse).

A procedure similar to that described above for zDHFR was used to clone human DHFR with His-tag (hDHFR-His) using the primer pair 5′-CCTCCCGCTGCTCATATGGTTGGTTCG-3′ (forward) and 5′-CTAGAAAACACCTTCCTCGAGATCATTCTTCTCATATA-3′ (reverse). The restriction enzyme sites for NdeI and XhoI, respectively, were introduced for the convenience of subsequent cloning. Successful cloning of all complete DHFR coding sequences was confirmed by restriction enzyme digestion and

Downloaded from dmd.aspetjournals.org at Kaohsiung Med Univ Lib on March 20, 2012

DMD DRUG METABOLISM AND DISPOSITION aspet

DNA sequencing. The resulting constructs were transformed into Rosetta (DE3) cells for expression and purification.

Expression and Purification of Recombinant DHFRs. *E. coli* containing the desired plasmid, zDHFR/pET43.1a, zDHFR-His/pET43.1a, or hDHFR-His/pET43.1a, was grown overnight at 37°C in 20 ml of Luria broth containing 100 μg/ml ampicillin. This culture was used to inoculate 300 ml of the same broth, and the inoculum continuously grew at 37°C. DHFR was induced by adding IPTG to a final concentration of 0.1 mM when the inoculum reached log phase. After 4 h of incubation with vigorous shaking at 25°C, bacteria cultures were centrifuged, and cell pellets were subjected to DHFR purification.

The induced zDHFR without His-tag was purified with the freeze/thaw cycling method development by Johnson and Hecht (1994) with slight modification. In brief, the cell pellet from the 200-ml culture was quickly immersed in ethanol bath at −80°C and completely frozen for at least 1 h before being removed from the freezer and slowly thawed on ice. This freeze/thaw step was repeated four times, and the frozen cell pellet from the last cycle was stored at −80°C until use. For purification, the frozen pellet was thawed on ice for 30 min, and 4 ml of 10 mM phosphate buffer, pH 7.5, containing 10 mM 2-mercaptoethanol was added to the pellet. The cell slurry was incubated on ice for another hour before centrifugation at 10,000*g* for 10 min at 4°C. The supernatant, containing the overexpressed DHFR, was carefully removed to another clean tube. Protamine sulfate was added to the supernatant to a final concentration of 4.5 mg/ml and mixed thoroughly. After centrifugation, the supernatant was applied to DEAE-Sephadex (2 × 5 cm; GE Healthcare, Chalfont St. Giles, UK), and zDHFR flowed through the column as a delayed major peak, as judged from the absorbance at 280 nm. Factions from the last-half portion of the peak were combined, and the enzyme was precipitated by 90% ammonium sulfate. The enzyme was resuspended in a minimal volume of 10 mM phosphate buffer and briefly dialyzed before storage.

For the purification of zDHFR-His, cells were resuspended in 6 ml of 50 mM Tris-HCl, pH 8.0, containing 2 mM EDTA, and lysed by adding 1 mg of lysozyme to the suspension. After a 15-min incubation at 4°C, the DNA in the lysate was removed by adding protamine sulfate and centrifugation. The clear supernatant was removed to a clean tube and mixed with a 2-fold volume of buffer A (20 mM sodium phosphate, pH 7.4, with 0.5 M NaCl and 20 mM imidazole). Approximately 5 ml of nickel-Sepharose resin slurry was pre-equilibrated with buffer A and mixed continuously and gently at 4°C for 1 h. The unbound protein was removed by centrifugation and five repetitive washes with a 5-fold volume of 50 mM imidazole in buffer A. zDHFR-His fusion protein was eluted with 200 mM imidazole in buffer A, precipitated by 60% ammonium sulfate, and stored at −80°C after brief dialysis.

A similar procedure for purifying zDHFR-His was used to express and purify human DHFR-His fusion protein (hDHFR-His), with minor modifications noted below. After protein bound to nickel-Sepharose, the resin was washed only with buffer A repetitively, and hDHFR-His was eluted with buffer A containing 150 mM imidazole. Also, we used Amicon Ultra-15 centrifugal filter devices (NMWL 10K; Millipore), instead of ammonium sulfate, to concentrate hDHFR-His. It is important to keep DHFR in solution containing 20% ammonium sulfate during the process of Amicon concentration to maintain the maximal stability and activity of the enzyme.

All purified DHFRs were stored at a concentration of 2 mg/ml in the presence of 5 mM 2-mecaptenethenal, 20% ammonium sulfate, and 10% sucrose at −80°C without significant loss of activity for at least 6 months. The purified zDHFR was subjected to subsequent analysis and polyclonal antibody production.

Determination of Stoichiometry for Human and Zebrafish DHFRs. DHFRs were chromatographed on a Superdex 200 exclusion column (0.46 × 30.0 cm) equilibrated with 20 mM potassium phosphate, pH 7.0, containing 100 mM NaCl and 5 mM 2-mercaptoethanol on an Agilent 1100 HPLC. The retention volume of DHFR was compared with the following standards: apoferritin (443 kDa), β-amylase (200 kDa), alcohol dehydrogenase (150 kDa), albumin (66 kDa), carbonic anhydrase (29 kDa), and ribonuclease A (14 kDa).

Measurements of DHFR Activity. DHFR irreversibly converts dihydrofolate and NADPH to tetrahydrofolate and $NADP^+$. The rate of tetrahydrofolate formation can be continuously monitored by the absorbance change at 340 nm (ε = 11,800 $M^{-1}cm^{-1}$), which corresponds to the decrease of NADPH and dihydrofolate (Stone and Morrison, 1986). An assay contained, in 1 ml, 20 mM Tris-HCl, pH 7.0, 0.5 M KCl, 100 μM NADPH, and 1 μg of DHFR. Reaction was initiated by adding various amounts of dihydrofolate to the final concentrations indicated in figures and legends. One unit DHFR activity was defined as the amount of enzyme required for converting 1 μmole of dihydrofolate to tetrahydrofolate in 1 min at 25°C.

The effects of chaotropic agents on DHFR activity were studied by measuring the initial velocity in 20 mM Tris-HCl, pH 7.0, containing saturated substrates (100 μM NADPH and 65 μM dihydrofolate), 1 μg of DHFR, and various concentrations of KCl or urea. The pH-dependence of DHFR activity was determined by measuring the initial velocity in buffer systems at constant ionic strength but various pH values. They contained 20 mM sodium acetate for pH 3.55 to 5.9, 20 mM potassium phosphate for pH 5.9 to 8.1, and 20 mM Tris-HCl for pH 7.0 to 10.14. All the above buffers contained 0.5 M KCl. Initial velocity was determined as preciously described except that the enzymes were preincubated with buffer and NADPH for 5 min before addition to the cuvette.

Inhibition of initial velocity was determined in a 1-ml cuvette containing 20 mM Tris-HCl, pH 7.0, and 0.5 M KCl. DHFR, 1 μg, was preincubated with NADPH and inhibitor at various concentrations at 25°C for 5 min before addition to the cuvette. Reactions were initiated by adding dihydrofolate to a final concentration of 60 μM. For monitoring the inhibitory effect of methotrexate, 86 μM dihydrofolate and 2 μg of DHFR were used. Most of the inhibitors were dissolved in dimethylsulfoxide and diluted in 20 mM Tris-HCl buffer with adjusted pH. The concentrations of inhibitors were determined using the extinction coefficients listed below: $\varepsilon_{272\ nm}$ = 6310 $M^{-1}cm^{-1}$ for trimethoprim, $\varepsilon_{295\ nm}$ = 4508.33 $M^{-1}cm^{-1}$ for EGCG, and $\varepsilon_{302\ nm}$ = 22,100 $M^{-1}cm^{-1}$ for methotrexate. Catechin and GSE concentrations were calculated using the exact amounts and molecular weight, if available. The use of 10 μl of 1% dimethylsulfoxide in the place of inhibitor was performed for the basal line determination. Percentage of activity remaining was determined by dividing the activity with inhibitor by that with dimethylsulfoxide, then multiplying by 100.

Fish Tissue Homogenization. Tissues or organs, including brain, eye, heart, liver, gastrointestinal tract, and muscle, were obtained from adult zebrafish after the animals were euthanized by waterborne exposure to tricaine (ethyl 3-aminobenzoate, methanesulfonic acid; Sigma-Aldrich). Tissues were rapidly isolated, stored in phosphate-buffered saline, and kept on ice during the whole process of extraction. Homogenization was carried out in the phosphate-buffered saline lysis buffer containing a protease inhibitor cocktail and RNase inhibitor (Sigma-Aldrich). Homogenized samples were centrifuged to remove particulate matters. Aliquots of the supernatant were subjected to Western blot and RT-PCR. The handling and disposition of fish tissues had been performed following the protocols approved by the Institutional Animal Care and Use Committee, National Cheng Kung University, Taiwan. The dominant yolk proteins in embryos before 24 hpf were removed as previously described to avoid interference (Link et al., 2006).

Western Blot Analysis. Protein content in a supernatant was determined using the Bradford and BCA methods. Proteins, 20 μg, were separated on a 10% SDS-separating gel and transferred to a PVDF membrane. After blocking overnight, the membrane was probed with anti-zDHFR antibody (1:1000 to 1:5000) prepared from purified zDHFR and then horseradish peroxidase-conjugated secondary antibody (1:5000). The PVDF membranes were also probed with anti-actin antibody for a loading control. The membrane was visualized using the SuperSignal chemiluminescent horseradish peroxidase substrate system from Pierce on an LAS-3000 imaging system (Fujifilm, Tokyo, Japan). In the case of the gastrointestinal tract, where the signal for actin was not detectable, Coomassie Blue staining was used to verify equal loading.

RT-PCR Analysis. We performed RT-PCR to determine the levels of DHFR transcripts. Total RNA was isolated from tissues with a TRIzol kit (Invitrogen) following the manufacturer's protocol. After isolation, 1 μg of total RNA from each tissue sample was reverse-transcribed with a high-capacity cDNA archive kit (Promega, Madison, WI), and 1 μl of the newly synthesized first-strand cDNA library was used as a template in the subsequent PCR analysis. The primers, 5′-CAGAAGATGACCATGACCCCTTCAG-3′ (forward) and 5′-GCTTGAGGATGCGGGTTACAAAC-3′ (reverse), for amplifying zDHFR reside in exons 2 and 5 of the zDHFR gene, respectively. The

Downloaded from dmd.aspetjournals.org at Kaohsiung Med Univ Lib on March 20, 2012

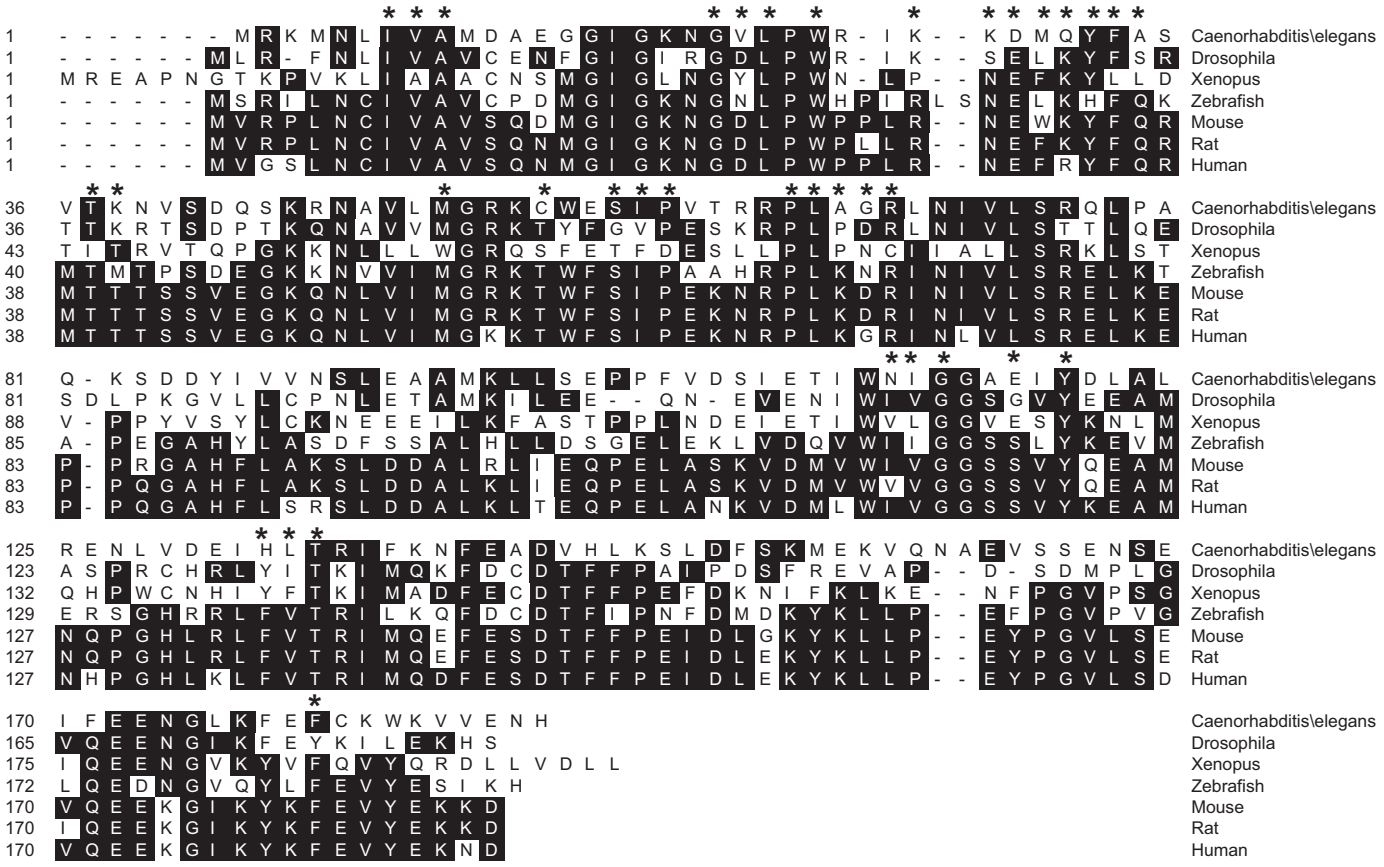

FIG. 2. Alignment of DHFR peptide sequences. The shaded characters indicate identical amino acids. Gaps, indicated by hyphens, are introduced for optimal alignment. The asterisks indicate the conserved amino acid residues surrounding the active site and substrate binding sites of the enzyme. The sequences were aligned using the Clustal W method (Combet et al., 2000) with MegAlign/DNAStar sequence analysis software (DNASTAR, Madison, WI). The GenBank accession numbers are: *Caenorhabditis elegans* DHFR, CAB02272; *Drosophila* (*Drosophila melanogaster*) DHFR, P17719; *Xenopus* (*Xenopus tropicalis*) DHFR, NP_001037882; mouse DHFR, CAA39544; rat DHFR, Q920D2; zebrafish DHFR, EU145591; human DHFR, EU145592.

primers 5′-AGACATCAAGGAGAAGCTGTG-3′ (forward) and 5′-TCCACGACGGAGTATTTAC-3′ (reverse) were for amplifying β-actin (391-bp fragment) as a control for RNA isolation and reverse-transcription. The annealing temperatures were 60°C for zDHFR and 62°C for β-actin, respectively. The PCR reaction condition was 30 cycles of 30 s at 94°C, 30 s at annealing temperature, and 68°C for 30 s.

Results

Sequence and Structural Analysis of Recombinant zDHFR. The full-length isolated zDHFR cDNA (EU145591) is 570 bp and encodes a protein of 190 amino acids. The primary sequence of cloned zDHFR is identical to that translated from the zDHFR online coding sequence (BC071330) (Fig. 2). Comparison between zebrafish DHFR and that from other species indicates conservation during evolution. A high level of homology is observed in the primary sequences and more so for the amino acid residues comprising the active site (Fig. 2). This strong homology in primary structure was reflected in the cross-reaction between anti-zDHFR antibody and human DHFR (data not shown). The primary structure of zDHFR is 58 and 63% identical to human and mouse DHFRs, respectively. An 86% identity between zebrafish and human DHFRs was observed within the amino acid residues composed of the active and substrate binding sites, including Ile^{7}, Phe^{36} (equivalent to Phe^{34} in hDHFR), and Leu^{69} (equivalent to Leu^{67} in hDHFR) (Bertino et al., 1987). Leu^{33} (equivalent to Phe^{31} in hDHFR), located in the dihydrofolate binding site and presumably interacting with the end of folate substrates and antifolate inhibitors, is present in zebrafish enzyme. Lys^{56} (Lys54 in hDHFR), the residue essential for NADPH binding, is also observed in zDHFR (Huang et al., 1990). Furthermore, Leu^{22}, Glu^{30}, and Ser^{118}, the critical residues involved in the up-regulation of DHFR protein levels by binding to their own mRNA upon methotrexate treatment, are conserved (Skacel et al., 2005). The primary sequence of zDHFR was subjected to online secondary structure prediction and compared with human DHFR [PredictProtein, http://www.predictprotein.org/newwebsite/submit-.php (Rost et al., 1996)]. The predicted three helices and seven strands of zDHFR were overlapped with those of hDHFR, indicating structural resemblance between zebrafish and human enzymes (Fig. 3).

Expression and Purification of DHFRs. The recombinant DHFRs were induced by adding 0.1 mM IPTG at 25°C for 4 h. The majority of induced DHFRs remained in soluble fractions under this condition. Higher induction temperature or prolonged induction time increased the amount of induced enzymes but also increased the ratio of insoluble and soluble DHFRs (data not shown). For zDHFR-His and hDHFR-His, the C-terminal His-tag allows us to use nickel-Sepharose and greatly simplifies the purification. The DHFR eluted from the nickel-Sepharose column was at least 95% pure, as judged from SDS-PAGE (Fig. 4). Approximately 4 mg of purified DHFRs were obtained from 200 ml of cells (Table 1).

To exclude the possible interference caused by the C-terminal His-tag, we also cloned zDHFR without His-tag and purified the enzyme using a modified freeze/thaw cycling method combined with DEAE-Sephadex chromatography. To date, most protocols for DHFR purification include the step of eluting the enzyme from a folate-

DMD DRUG METABOLISM AND DISPOSITION aspet
Downloaded from dmd.aspetjournals.org at Kaohsiung Med Univ Lib on March 20, 2012

DMD DRUG METABOLISM AND DISPOSITION aspet

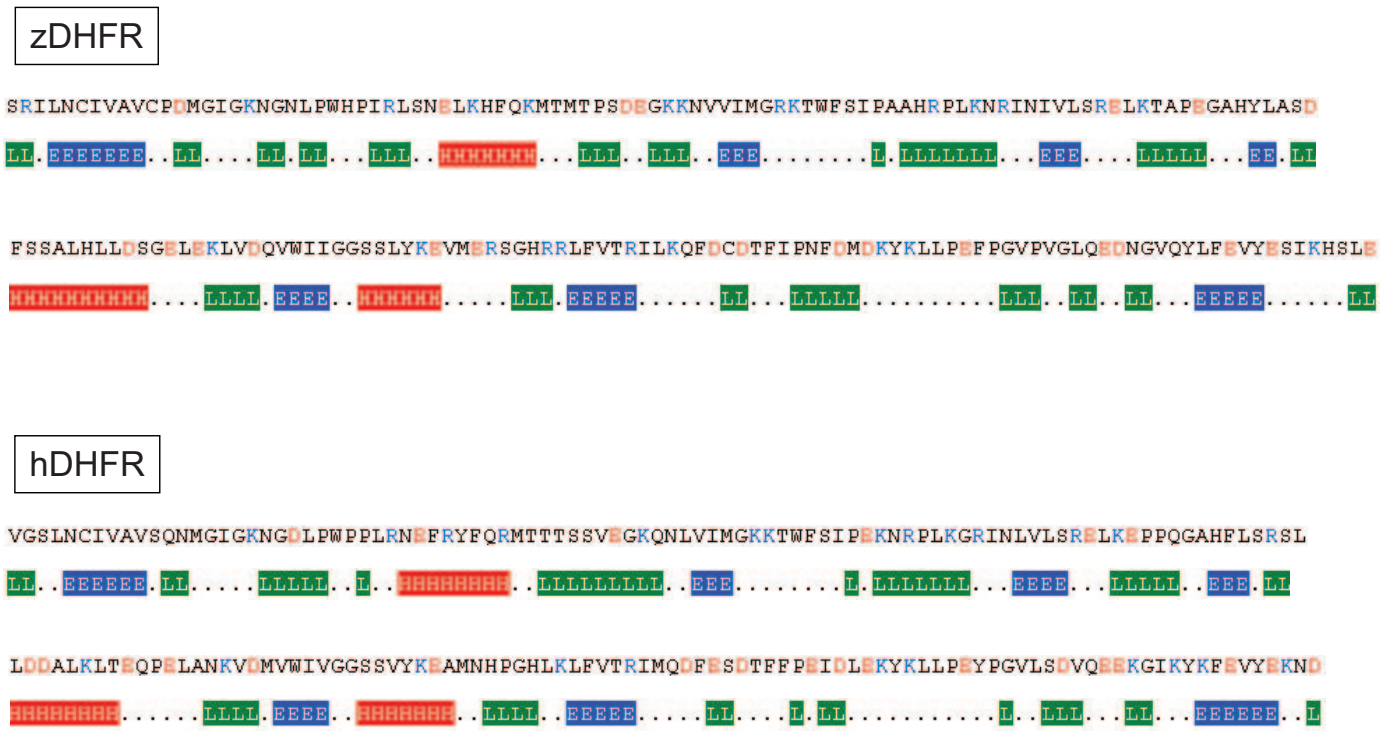

FIG. 3. Comparison of predicted zebrafish and human DHFR secondary structures. Primary sequences of both zDHFR (upper panel) and hDHFR (lower panel) were analyzed with online software for the secondary structure arrangement (Rost and Sander, 1993; Rost et al., 1996). H in red block, helix; E in blue block, strand; L in green block, neither helix nor strand.

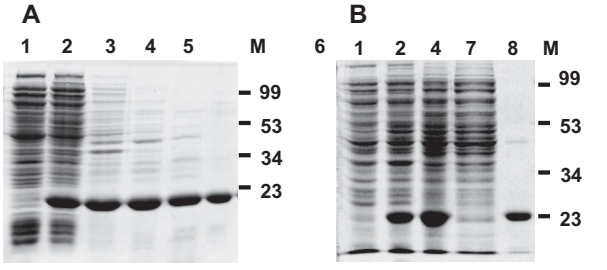

FIG. 4. SDS-PAGE of zDHFR (A), zDHFR-His (B), and hDHFR-His (C) at each step of purification. Lane 1, uninduced cell lysate; lane 2, IPTG-induced cell lysate; lane 3, supernatant after freeze/thaw cycles; lane 4, after DNA removal by protamine sulfate precipitation; lane 5, after 50~90% ammonium sulfate precipitation; lane 6, after DEAE-Sephadex; lane 7, unbound fraction from nickel-Sepharose; lane 8, DHFR eluted from nickel-Sepharose; M, molecular weight marker.

affinity column with high concentrations of folic acid. Additional steps are hence required to remove folic acid, which is often time-consuming and sometime deleterious to the enzyme. The three consecutive cycles of freeze/thaw in our purification released most of the induced enzyme into the extracellular fraction where zDHFR was estimated to be 70 to 80% of the total protein (Fig. 4). However, the original freeze/thaw method developed by Johnson and Hecht (1994) poses a difficulty, because the dry ice used to freeze cells is not always available to us. To overcome this obstacle, we used an ethanol bath at −80°C to freeze cell pellets and obtained satisfactory results. We believe this minor modification should have alleviated the drawback and increased the feasibility of the freeze/thaw method. In addition, subsequent use of DEAE-Sephadex avoided the steps for folic acid removal and significantly sped up the purification. Starting from the last cycle of freeze/thaw, we were able to obtain 3 mg of ready-to-use recombinant zDHFR from 200 ml of culture cells in 3 h with great yield and purity.

Quaternary Structure of zDHFRs. Additional evidence supporting the structural resemblance between human and zebrafish DHFR is their monomeric quaternary structures. Native zDHFR-His had a Stokes radius close to a globular protein of 20 kDa and was eluted at the same retention volume as the human enzyme (data not shown). This result indicates a monomeric structure for recombinant zebrafish DHFR and is in agreement to the previous report for human DHFR (Jarabak and Bachur, 1971). The C-terminal His-tag did not affect DHFRs in their quaternary structures as well as all properties described below.

Analysis of zDHFR Enzymatic Activity. Both the apparent K_m for dihydrofolate and K_{cat} of zDHFR are comparable with the values for hDHFR. We determined DHFR activity by continuously monitoring the absorbance decrease at 340 nm, which corresponds to the decrease of NADPH. Double-reciprocal plots of initial velocity versus dihydrofolate concentration permit the determination of apparent K_m for dihydrofolate and K_{cat} (Fig. 5). The estimated K_m of zDHFR for dihydrofolate is 3.3 μM. This value is within the range of 0.036 to 5.9 μM, the K_m reported for human DHFR (Delcamp et al., 1983) The estimated K_{cat} of zDHFR for dihydrofolate is 435 min^{-1}. This value is also comparable with the K_{cat} of human (518 min^{-1}) and rat (380 min^{-1}) enzymes (Jarabak and Bachur, 1971). Folic acid was a less effective substrate for zDHFR as compared with dihydrofolate. We observed an approximately 30-fold decrease in zDHFR K_{cat} when folic acid was used as substrate (data not shown).

Two pH optima, approximately 6.0 and 7.5, were observed for zDHFR dihydrofolate reduction activity. These two pH values are

Downloaded from dmd.aspetjournals.org at Kaohsiung Med Univ Lib on March 20, 2012

TABLE 1

Purification of zDHFR and hDHFR expressed in E. coli Rosetta cells

Purification Step	Volume	Protein	Specific Activity	Yield	Purification (-Fold)
	ml	*mg*	*units/mg*	*%*	
ZDHFR					
F/T cycle	6	25	5	100	1.0
Protamine sulfate	7	20	6	93	1.2
50 to 90% AS[a]	1	12	7	69	1.4
DEAE-Sephadex	3	3	8	18	1.6
zDHFR-His					
Crude cell extract[b]	2	31	6	100	1.0
Ni^{2+}-Sepharose	1.5	4	13	26	2.2
hDHFR-His					
Crude cell extract[b]	1	43	1	100	1.0
Ni^{2+}-Sepharose	4	4	6	54	6.0

AS, ammonium sulfate; F/T, freeze/thaw.
[a] Resuspended protein pellet after 90% AS precipitation.
[b] Extract after protamine sulfate precipitation.

comparable with those reported for the human enzyme (data not shown) (Jarabak and Bachur, 1971). Less than 10% decrease in zDHFR activities was observed after a 1-h incubation of enzyme in the solutions of pH 6.0 and 7.5 (data not shown).

One of the well documented properties of human DHFR is activation by chaotropic agents (Jarabak and Bachur, 1971). The activation patterns of zDHFR by KCl and urea were similar to that of the human enzyme with approximately 2- to 5-fold activation observed in the presence of 0.5 M KCl or 2 M urea (data not shown).

Inhibition of zDHFR Activity. Inhibitory patterns of DHFR activity by compounds against this enzyme are also comparable between recombinant zebrafish and human DHFRs. Dihydrofolate reduction, catalyzed by both recombinant zebrafish and human DHFRs, was completely inhibited by methotrexate at the final concentration of approximately 60 nM (Fig. 6A). Trimethoprim, a selective inhibitor of microbial DHFR with a 50,000-fold selectivity for bacterial DHFR over human enzyme, also inhibited zDHFR with an IC_{50} close to 10 μM (Fig. 6B) (Roth et al., 1987). Although zDHFR is approximately 7-fold more sensitive than hDHFR to trimethoprim inhibition, this difference is considered insignificant when compared with the 50,000-fold higher sensitivity of bacterial DHFRs to trimethoprim. As mentioned previously, folic acid is a less effective substrate of DHFR. The presence of folic acid in the reaction mixture repressed the conversion of dihydrofolate to tetrahydrofolate with an IC_{50} of 20 μM. Approximately 80% inhibition was observed when the final concentration of folic acid was brought to 70 μM or higher (Fig. 6C).

GSE also significantly inhibited DHFR-mediated dihydrofolate reduction. The IC_{50} of GSE to zebrafish and human DHFR activities was approximately 2 μg/ml for both (Fig. 6D). GSE contains lipids, protein, carbohydrates, and polyphenols including catechins and EGCG. Both zDHFR and hDHFR were inhibited by EGCG to a similar extent, with the IC_{50} values close to 100 μM (Fig. 6E). We did not observe any change in the initial velocity of dihydrofolate reduction when catechin was added to the assay, suggesting that catechin did not contribute to the inhibitory activity of GSE (Fig. 6F). Less than 3% inhibition of DHFR activity was observed when dimethylsulfoxide, the solvent used to dissolve inhibitors, was added to the reaction for basal line inhibition determination (data not shown). No significant difference was observed in the inhibitory activities of all above-mentioned compounds with or without the presence of the chaotropic agent KCl (data not shown).

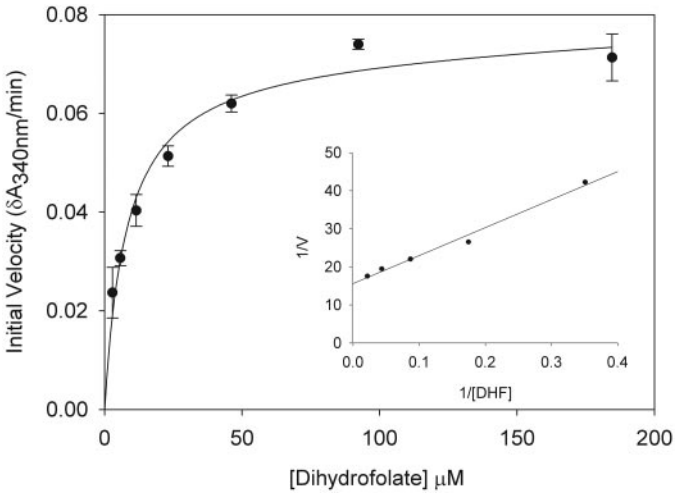

FIG. 5. Kinetics of dihydrofolate conversion to tetrahydrofolate catalyzed by zDHFR. Zebrafish DHFR activity was monitored by the absorbance decrease at 340 nm. Reactions were carried out in a 1-cm cuvette containing 20 mM Tris-HCl, pH 7.0, 0.5 M KCl, 100 μM NADPH, and 1 μg of DHFR at 25°C on a Helios thermo spectrophotometer. Reactions were started by adding substrate dihydrofolate to final concentrations ranging from 2.8 to 184.5 μM. Inset shows the reciprocal plot of initial velocity versus dihydrofolate concentration, yielding apparent K_{cat} of zDHFR and K_m for dihydrofolate.

Tissue-Specific and Stage-Dependent Expression of zDHFR. We examined DHFR distribution among tissues and embryos of different developmental stages with Western blot and RT-PCR. Significant levels of DHFR protein were detected only in brain and liver, indicating tissue-specific expression in zebrafish (Fig. 7). Nevertheless, post-transcriptional regulation might also play a role in controlling intracellular levels of DHFR, since DHFR mRNA was evenly distributed among all tissues examined. We noticed that appreciable amounts of DHFR protein were also found in unfertilized eggs, implying an important role of this enzyme in early embryonic development. This speculation was further supported by our observation that DHFR protein was abundant in the embryos up to 3 days post-fertilization (dpf) but abruptly diminished after 4 dpf. Equal abundance of mRNA observed in embryos of all stages also supports our hypothesis of post-transcriptional regulation of DHFR protein distribution (Fig. 8).

Discussion

In the present study, we cloned and characterized DHFR from zebrafish, a prominent animal model for studies in embryogenesis and drug discovery. Currently, no in vivo evidence or comparison has been reported to show the comparability between human and zebrafish DHFRs. However, the in vitro studies on the primary sequences, predicted secondary structures, and quaternary structures reveal considerable similarity between zebrafish and human DHFRs. Resemblance between the two orthologous enzymes was also observed in their catalytic properties, kinetic constants, activation patterns by chaotropic reagents, and susceptibility to inhibitors. Zebrafish DHFR seems to follow Michaelis kinetics with respect to varying dihydrofolate concentrations. This is similar to the DHFR purified from human placenta (Jarabak and Bachur, 1971) but different from mouse enzyme, where a sigmoid substrate saturation curve was observed (McCullough and Bertino, 1971). The susceptibilities to methotrexate and trimethoprim inhibition were also comparable between human and zebrafish DHFRs, offering a promising alternative for antifolate drug research.

DHFR was highly expressed in zebrafish ova and embryos of early

DMD DRUG METABOLISM AND DISPOSITION aspet
Downloaded from dmd.aspetjournals.org at Kaohsiung Med Univ Lib on March 20, 2012

DMD DRUG METABOLISM AND DISPOSITION aspet

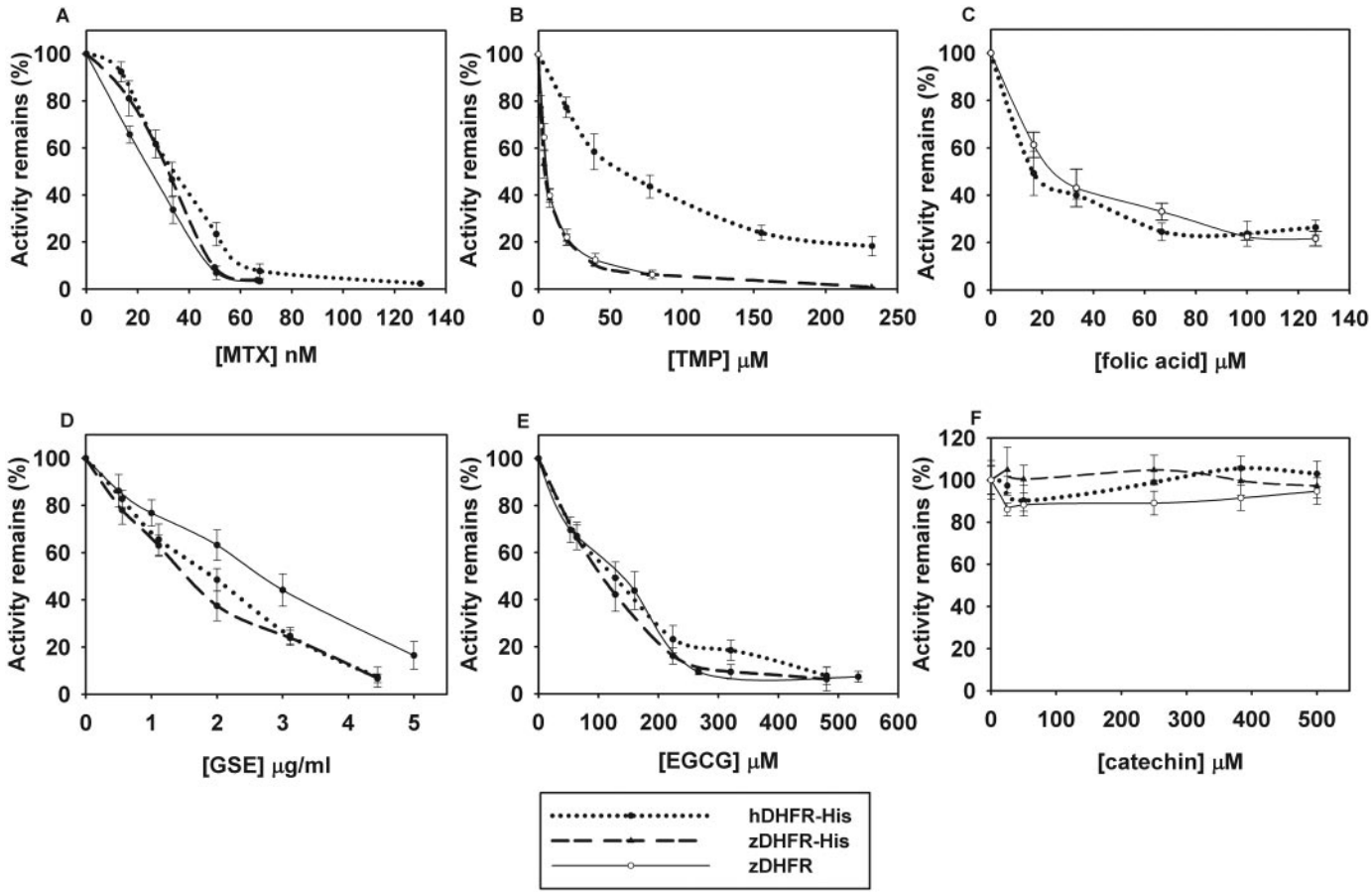

FIG. 6. Inhibition of DHFR activity by known and potential antifolate agents. Inhibition on initial velocity of DHFR-catalyzed dihydrofolate reduction was determined at 25°C in the presence of methotrexate (A), trimethoprim (B), folic acid (C), GSE (D), EGCG (E), and (±)catechin (F) in the concentrations of indicated ranges. All assays contain 60 μM of dihydrofolate and 1 μg of DHFR except for methotrexate (B), where 76 μM of dihydrofolate and 2 μg of enzyme were used. All assays were performed in buffer containing 0.5 M KCl except catechin (F), where no KCl was added. MTX, methotrexate; TMP, trimethoprim.

stages, suggesting a crucial role of this enzyme in embryonic development. An abrupt decrease in DHFR protein level was observed in embryos between 3 and 4 dpf. That is when a developing embryo has completed most of its morphogenesis and evolved as a swimming larva (Kimmel et al., 1995). Our results are in agreement with the observation that DHFR activity was significantly increased in the early stages of mammalian embryos (Roberts and Hall, 1965). We expected to see high levels of DHFR remaining in larva after 3 dpf, where cells still proliferate rapidly and lots of folates are supposedly required, as in rapidly proliferating cancer cells. However, no appreciable amounts of DHFR protein were found in hatched larva. One possible explanation is that DHFR is involved more in differentiation regulation than in cell growth during embryogenesis. Support for this speculation is a recent study showing that a DHFR knockdown causes cardiac malformation in zebrafish (Sun et al., 2007). We are convinced that it is important to distinguish the role and regulatory mechanism of DHFR in rapidly proliferating cells of embryos, which is "natural and well controlled," from that of cancer, which is "malignant and out-of-control." The studies to determine whether this enzyme is involved in cell regulation and is not simply a "housekeeping gene" are also warranted.

The highest expression of DHFR was found in the brain among all tissues examined. This is in contrast to the previous reports for rabbit that DHFR activity in brain extracts was only 10 to 18% of that in liver extracts (Spector et al., 1977). This difference might reflect the variation among species. In humans, DHFR activity was found to be low in fetus and barely detectable in most normal adult tissues (Whitehead et al., 1987). A significant level of DHFR protein was also observed in zebrafish liver but not detected in the gastrointestinal tract. This result supports the recently revised hypothesis that liver, instead of intestine, is the initial primary site for folic acid metabolism (Wright et al., 2005). DHFR protein and mRNA levels of the same tissue did not always coincide, especially in the heart, suggesting that post-transcriptional and/or post-translational regulation might play a role in controlling the intracellular concentrations of zDHFR. Enzyme stabilization by the binding of folate substrates and/or cofactors has been observed for many folate enzymes, including DHFR (Junker et al., 2005).

We showed in the present study that folic acid inhibits DHFR reduction to dihydrofolate. It is becoming increasingly evident that folate possesses dual modulatory effects on the development of diseases, depending on when and how much is ingested (Kim, 2007). Our results reveal the possibility that the excess unmetabolized folic acid, probably from a high-dose and long-term folate supplement, may interfere with dihydrofolate recycling during dTMP and DNA biosynthesis, as well as with folate-mediated one-carbon metabolism, especially in brain. Future in vivo experiments in zebrafish will help to determine potential detrimental effects of unmetabolized folic acid in folate-mediated one-carbon metabolism.

We showed that EGCG, one of the polyphenols rich in green tea and GSE, inhibits both zDHFR and hDHFR to a comparable extent, in agreement with a recent study showing that EGCG disrupted the

Downloaded from dmd.aspetjournals.org at Kaohsiung Med Univ Lib on March 20, 2012

DMD
DRUG METABOLISM AND DISPOSITION
aspet

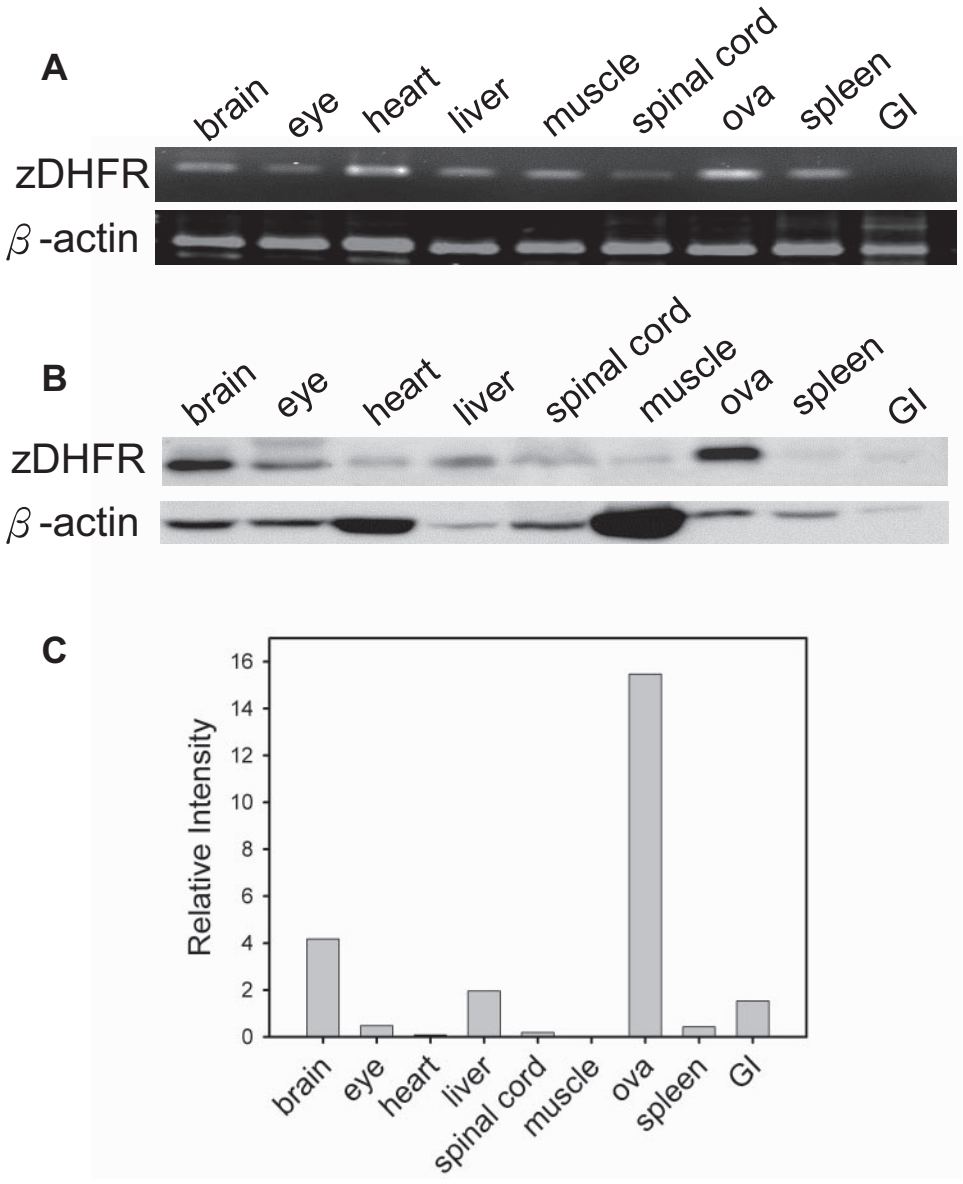

FIG. 7. Tissue-specific distribution of zebrafish dihydrofolate reductase. Individual tissues from adult female zebrafish were prepared for RT-PCR (A) and Western blot analysis (B) as described in *Materials and Methods*. C, the abundance of DHFR protein in individual tissues was normalized by dividing the signal intensity of bands corresponding to DHFR by that of β-actin. The signal intensity was quantified using the image analytic software Multi Gauge 2.01 (Fujifilm). Results presented here are representative of six independent repeats. GI, gastrointestinal track.

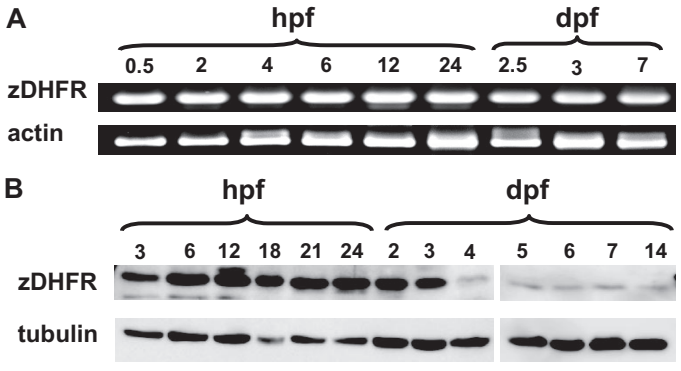

FIG. 8. Stage-dependent expression of zebrafish dihydrofolate reductase. Embryos of indicated stages were collected and applied to RT-PCR using actin as internal control (A) and Western blot analysis using tubulin as loading control (B) after proper extraction and preparation as described in *Materials and Methods*. All the embryos in the stages earlier than and including 24 hpf were deyolked before being subjected to analysis. Results presented here are representative of five independent repeats.

folate cycle (Navarro-Peran et al., 2007). However, (±)catechins, another component also identified in GSE, showed no effect on DHFR activity. This is in agreement with the observation that the ester bound gallate moiety is essential for DHFR inhibitory activity (Navarro-Peran et al., 2005). Recently, GSE has been marketed as a dietary supplement owing to its beneficial effects, including inhibiting cancer cell proliferation (Raina et al., 2007). The DHFR inhibitory activity of GSE unveiled in this study provides an additional mechanism for the antiproliferative activity of GSE and supports the chemopreventive and antimicrobial potentials of this compound. However, the antifolate activity of GSE may also lead to harmful effects in vivo due to the possible intervention in folate absorbance and metabolism along with other biochemical pathways. Proper safety measures are hence crucial when GSE is subjected to clinical uses.

Our studies show that zebrafish DHFR is similar to human enzymes and can serve as an in vitro system for antifolate drug analysis. Antifolates against DHFR remain an extremely important class of drugs for the treatment of various pathogeneses, including neoplastic and non-neoplastic diseases as well as microbial infections. Efforts to develop antifolate drugs with better efficacy will be continued in

Downloaded from dmd.aspetjournals.org at Kaohsiung Med Univ Lib on March 20, 2012

addition to determination of the functional mechanism of DHFR (Longo-Sorbello and Bertino, 2001). Zebrafish has attracted many researchers' interests in the past two decades. The advantages are its similarity to mammals in many biological pathways and pathogenesis, abundant offspring, external and rapid development, transparent embryo, and easy growth and breeding. Especially important for drug discovery is that zebrafish embryos are permeable to small molecules and drugs during organogenesis, providing easy access for drug administration and vital dye staining (Kari et al., 2007). The well established tools of molecular biology for gene manipulation have also significantly assisted the progress in this field. We have previously reported the appreciable similarity of two other zebrafish folate enzymes, mitochondrial and cytosolic serine hydroxymethyltransferases, to their human orthologs (Chang et al., 2006; Chang et al., 2007). We are convinced that zebrafish is comparable with human in folate-mediated one-carbon metabolism and will serve as a valuable animal model for folate-related studies and drug discovery.

References

Bertino JR, Sobrero A, Mini E, Moroson BA, and Cashmore A (1987) Design and rationale for novel antifolates. *NCI Monogr* **5:**87–91.

Chang WN, Tsai JN, Chen BH, and Fu TF (2006) Cloning, expression, purification, and characterization of zebrafish cytosolic serine hydroxymethyltransferase. *Protein Expr Purif* **46:**212–220.

Chang WN, Tsai JN, Chen BH, Huang HS, and Fu TF (2007) Serine hydroxymethyltransferase isoforms are differentially inhibited by leucovorin: characterization and comparison of recombinant zebrafish serine hydroxymethyltransferases. *Drug Metab Dispos* **35:**2127–2137.

Combet C, Blanchet C, Geourjon C, and Deleage G (2000) NPS@: network protein sequence analysis. *Trends Biochem Sci* **25:**147–150.

Delcamp TJ, Susten SS, Blankenship DT, and Freisheim JH (1983) Purification and characterization of dihydrofolate reductase from methotrexate-resistant human lymphoblastoid cells. *Biochemistry* **22:**633–639.

Gangjee A, Jain HD, and Kurup S (2007) Recent advances in classical and non-classical antifolates as antitumor and antiopportunistic infection agents: part I. *Anticancer Agents Med Chem* **7:**524–542.

Gisondi P, Fantuzzi F, Malerba M, and Girolomoni G (2007) Folic acid in general medicine and dermatology. *J Dermatolog Treat* **18:**138–146.

Huang S, Appleman R, Tan XH, Thompson PD, Blakley RL, Sheridan RP, Venkataraghavan R, and Freisheim JH (1990) Role of lysine-54 in determining cofactor specificity and binding in human dihydrofolate reductase. *Biochemistry* **29:**8063–8069.

Jarabak J and Bachur NR (1971) A soluble dihydrofolate reductase from human placenta: purification and properties. *Arch Biochem Biophys* **142:**417–425.

Johnson BH and Hecht MH (1994) Recombinant proteins can be isolated from E. coli cells by repeated cycles of freezing and thawing. *Biotechnology* **12:**1357–1360.

Junker JP, Hell K, Schlierf M, Neupert W, and Rief M (2005) Influence of substrate binding on the mechanical stability of mouse dihydrofolate reductase. *Biophys J* **89:**L46–L48.

Kari G, Rodeck U, and Dicker AP (2007) Zebrafish: an emerging model system for human disease and drug discovery. *Clin Pharmacol Ther* **82:**70–80.

Kim YI (2007) Folate and colorectal cancer: an evidence-based critical review. *Mol Nutr Food Res* **51:**267–292.

Kimmel CB, Ballard WW, Kimmel SR, Ullmann B, and Schilling TF (1995) Stages of embryonic development of the zebrafish. *Dev Dyn* **203:**253–310.

Link V, Shevchenko A, and Heisenberg CP (2006) Proteomics of early zebrafish embryos. *BMC Dev Biol* **6:**1.

Longo-Sorbello GS and Bertino JR (2001) Current understanding of methotrexate pharmacology and efficacy in acute leukemias. Use of newer antifolates in clinical trials. *Haematologica* **86:**121–127.

Markle HV (1997) Unmetabolized folic acid and masking of cobalamin deficiency. *Am J Clin Nutr* **66:**1480–1481.

McCullough JL and Bertino JR (1971) Dihydrofolate reductase from mouse liver and spleen. Purification, properties and inhibition by substituted 2,4-diaminopyrimidines and 4,6-diaminotriazines. *Biochem Pharmacol* **20:**561–574.

Miranda CL, Collodi P, Zhao X, Barnes DW, and Buhler DR (1993) Regulation of cytochrome P450 expression in a novel liver cell line from zebrafish (Brachydanio rerio). *Arch Biochem Biophys* **305:**320–327.

Navarro-Peran E, Cabezas-Herrera J, Garcia-Canovas F, Durrant MC, Thorneley RN, and Rodriguez-Lopez JN (2005) The antifolate activity of tea catechins. *Cancer Res* **65:**2059–2064.

Navarro-Peran E, Cabezas-Herrera J, Campo LS, and Rodriguez-Lopez JN (2007) Effects of folate cycle disruption by the green tea polyphenol epigallocatechin-3-gallate. *Int J Biochem Cell Biol* **39:**2215–2225.

Parle-McDermott A, Pangilinan F, Mills JL, Kirke PN, Gibney ER, Troendle J, O'Leary VB, Molloy AM, Conley M, Scott JM, et al. (2007) The 19-bp deletion polymorphism in intron-1 of dihydrofolate reductase (DHFR) may decrease rather than increase risk for spina bifida in the Irish population. *Am J Med Genet A* **143:**1174–1180.

Raina K, Singh RP, Agarwal R, and Agarwal C (2007) Oral grape seed extract inhibits prostate tumor growth and progression in TRAMP mice. *Cancer Res* **67:**5976–5982.

Roberts DW and Hall TC (1965) Studies on folic reductase. II. Enzyme activity of embryonic organs of the chicken, rat, and human. *Cancer Res* **25:**1894–1898.

Rost B and Sander C (1993) Prediction of protein secondary structure at better than 70% accuracy. *J Mol Biol* **232:**584–599.

Rost B, Fariselli P, and Casadio R (1996) Topology prediction for helical transmembrane proteins at 86% accuracy. *Protein Sci* **5:**1704–1718.

Roth B, Rauckman BS, Ferone R, Baccanari DP, Champness JN, and Hyde RM (1987) 2,4-Diamino-5-benzylpyrimidines as antibacterial agents. 7. Analysis of the effect of 3,5-dialkyl substituent size and shape on binding to four different dihydrofolate reductase enzymes. *J Med Chem* **30:**348–356.

Shi J, Yu J, Pohorly JE, and Kakuda Y (2003) Polyphenolics in grape seeds—biochemistry and functionality. *J Med Food* **6:**291–299.

Skacel N, Menon LG, Mishra PJ, Peters R, Banerjee D, Bertino JR, and Abali EE (2005) Identification of amino acids required for the functional up-regulation of human dihydrofolate reductase protein in response to antifolate treatment. *J Biol Chem* **280:**22721–22731.

Spector R, Levy P, and Abelson HT (1977) Identification of dihydrofolate reductase in rabbit brain. *Biochem Pharmacol* **26:**1507–1511.

Stone SR and Morrison JF (1986) Mechanism of inhibition of dihydrofolate reductases from bacterial and vertebrate sources by various classes of folate analogues. *Biochim Biophys Acta* **869:**275–285.

Sun SN, Gui YH, Wang YX, Qian LX, Jiang Q, Liu D, and Song HY (2007) Effect of dihydrofolate reductase gene knock-down on the expression of heart and neural crest derivatives expressed transcript 2 in zebrafish cardiac development. *Chin Med J* **120:**1166–1171.

Troen AM, Mitchell B, Sorensen B, Wener MH, Johnston A, Wood B, Selhub J, McTiernan A, Yasui Y, Oral E, et al. (2006) Unmetabolized folic acid in plasma is associated with reduced natural killer cell cytotoxicity among postmenopausal women. *J Nutr* **136:**189–194.

Westerfield M (1995) *The zebrafish book: guide for the laboratory use of zebrafish (Danio rerio)*. University of Oregon Press, Eugene.

Whitehead VM, Kamen BA, and Beaulieu D (1987) Levels of dihydrofolate reductase in livers of birds, animals, primates, and man. *Cancer Drug Deliv* **4:**185–189.

Wright AJ, Finglas PM, Dainty JR, Wolfe CA, Hart DJ, Wright DM, and Gregory JF (2005) Differential kinetic behavior and distribution for pteroylglutamic acid and reduced folates: a revised hypothesis of the primary site of PteGlu metabolism in humans. *J Nutr* **135:**619–623.

Address correspondence to: Tzu-Fun Fu, Department of Medical Laboratory Science and Biotechnology, College of Medicine, National Cheng Kung University, No. 1, University Road, Tainan 701, Taiwan. E-mail: tffu@mail.ncku.edu.tw

DMD DRUG METABOLISM AND DISPOSITION aspet

Downloaded from dmd.aspetjournals.org at Kaohsiung Med Univ Lib on March 20, 2012